



Published in final edited form as:

Bioorg Chem. 2020 September ; 102: 104079. doi:10.1016/j.bioorg.2020.104079.

Modulation of estrogen-related receptors subtype selectivity: Conversion of an ERR β/γ selective agonist to ERR $\alpha/\beta/\gamma$ pan agonists

Mohamed Shahien^a, Mohamed Elagawany^{b,c,d}, Sadichha Sitaula^c, Shaimaa S. Goher^a, Sheryl L. Burris^c, Ryan Sanders^c, Amer Avdagic^c, Cyrielle Billon^{b,c}, Lamees Hegazy^{b,c}, Thomas P. Burris^{b,c}, Bahaa Elgendy^{a,b,c,*}

^aChemistry Department, Faculty of Science, Benha University, Benha 13518, Egypt

^bDepartment of Pharmaceutical and Administrative Sciences, St. Louis College of Pharmacy, St. Louis, MO 63110, USA

^cCenter for Clinical Pharmacology, Washington University School of Medicine and St. Louis College of Pharmacy, St. Louis, MO 63110, USA

^dDepartment of Pharmaceutical Chemistry, Faculty of Pharmacy, Damanhour University, Damanhour, Egypt

Abstract

Estrogen Related Receptors (ERRs) are key regulators of energy homeostasis and play important role in the etiology of metabolic disorders, skeletal muscle related disorders, and neurodegenerative diseases. Among the three ERR isoforms, ERR α emerged as a potential drug target for metabolic and neurodegenerative diseases. Although ERR β/γ selective agonist chemical tools have been identified, there are no chemical tools that effectively target ERR α agonism. We successfully engineered high affinity ERR α agonism into a chemical scaffold that displays selective ERR β/γ agonist activity (**GSK4716**), providing novel ERR $\alpha/\beta/\gamma$ pan agonists that can be used as tools to probe the physiological roles of these nuclear receptors. We identified the structural requirements to enhance selectivity toward ERR α . Molecular modeling shows that our novel modulators have favorable binding modes in the LBP of ERR α and can induce conformational changes where Phe328 that originally occupies the pocket is dislocated to accommodate the ligands in a rather small cavity. The best agonists up-regulated the expression of target genes PGC-1 α and PGC-1 β , which are necessary to achieve maximal mitochondrial biogenesis. Moreover, they increased the mRNA levels of PDK4, which play an important role in energy homeostasis.

* Corresponding author.

Declaration of Competing Interest

The authors declare that they have no known competing financial interests or personal relationships that could have appeared to influence the work reported in this paper.

Appendix A. Supplementary material

Supplementary data to this article can be found online at <https://doi.org/10.1016/j.bioorg.2020.104079>.

Keywords

Estrogen-Related Receptors; Pan Agonists; Molecular Modeling; *N*-Acyl Hydrazones

1. Introduction

Estrogen Related Receptors (ERRs) are members of the nuclear hormone receptors (NRs) superfamily. The ERRs subfamily comprise three members, ERR α , ERR β and ERR γ ; and are closely related to the estrogen receptors (ER α and ER β). ERR α and ERR β were identified by Giguère and his co-workers in 1988 [1], and ERR γ was identified in 1999 by Chen et al. [2].

The ERRs are orphan receptors since no natural ligands have been identified for any of the three ERR isoforms. Unlike ERs, ERRs have constitutive activity and can function in absence of ligands. Although ERRs are structurally related to ERs and share sequence similarity with these receptors, they do not bind with estrogens, which are the endogenous ligands of the ERs. ERR α is expressed mainly in tissues of high energy demand such as brown adipose tissue, intestine, and skeletal muscles and functions as a sensor of energy metabolism. ERR β is expressed in low levels in adult skeletal muscle, heart, kidney, eyes, and ears. This isoform is known to play an important role in the early development and its postnatal expression is highly restricted. ERR γ is expressed mainly in skeletal muscle, heart, pancreas, kidney, placenta, spinal cord and brain [3–5]. Within the ERR subfamily, ERR α is the most divergent of the $\alpha/\beta/\gamma$ trio, especially with regard to the ligand binding domain (LBD). The ligand binding pocket (LBP) of ERR α is only 100 Å³, which makes it the smallest LBP among NRs. ERR α is constitutively active because the LBP is partially filled with the amino acid residue Phe328, which allows helix 12 (H12) to adopt an active conformation that can interact with coactivators. The crystal structure of ERR α LBD in complex with coactivator PGC-1 α shows that estrogen-like ligands cannot fit the small LBP and most likely will disrupt the active conformation [6]. This is probably why the majority of ERR α identified ligands are inverse agonists. Co-crystal structure of inverse agonist **1** with ERR α LBD shows that only part of this ligand fits in the LBD and the rest of the ligand sticks out from the LBP. The LBP undergoes significant conformational changes to accommodate the ligand and Phe510 (on H12) was dislocated to avoid steric clash with Phe328. Consequently, H12 was displaced to fill the coactivator groove of the AF-2 and therefore inactivate the receptor. This molecular mechanism is unique to ERR α and highlights the possibility of rationally designing drugs to modulate ERR α despite the small size of the LBP. Even though ERR α LBP is small in size and partially filled, a well-designed small-molecule ligand can be accommodated if it can promote conformational changes and cause the cavity to open up.

Several ERR α inverse agonists have been identified. Kaempferol (**2**), dietary flavonol found in many natural products, can reduce gene transcription by inhibiting the interaction between ERR α and DNA response elements [7]. XCT790 (**3**) is another ERR α inverse agonist that works by inducing ERR α ubiquitin-dependent proteasomal degradation [8,9]. This compound can inhibit the proliferation of A549 lung cancer cell [10] and HepG2

hepatocarcinoma and its multi-drug resistance (MDR) sub-line R-HepG2 by inducing mitochondrial reactive oxygen species [11] and reducing mitochondrial mass. XCT790 (**3**) reduces the expression of PGC-1 α [12] and PGC-1 β [13], thus suppressing mitochondrial biogenesis and increasing glucose uptake.

Scientists at GlaxoSmithKline suggested that ERR α may be intractable as a drug target after they failed to identify ERR α agonists using high-throughput screening and structure guided design [14]. However, natural phytoestrogens were identified by virtual screening as potential ERR α agonists. For example, in addition to functioning as ER α and ER β agonists, genistein (**4a**), daidzein (**4b**), and biochanin (**4c**) are three isoflavones, which behaved as agonists for all ERRs and were shown to activate ERR α in mammalian cell transfection and mammalian two-hybrid experiments [15].

Ding et al. identified a series of pyrido[1,2-*a*]pyrimidin-4-ones as ERR α agonists by screening their carbonyl focused library [16]. These compounds enhanced the uptake of glucose and fatty acid in C2C12 muscle cells through the elevation of mRNA and protein levels of ERR α in downstream targets. Compound **5** has an agonistic effect on ERR α and was shown to increase the transcription of ERR α in a dose dependent manner. Moreover, compound **5** activated the receptor in 293FT cells pretreated with kaempferol (**2**), which is known inverse agonist of ERR α . Interestingly, **5** increased the mRNA levels of key target genes involved in oxidative metabolism such as MCAD, PDK4, and ATP5b. This compound was selective for ERR α over ER α , ER β , and ERR β . However, **5** moderately agonized ERR γ [16].

As part of our ongoing research program to develop chemical tools for various nuclear receptors (e.g. LXR [17–20], ROR [21], REV-ERB [22]), we became interested in developing ERR α / γ dual agonists with the aim of eventually developing small molecule agonists specific to ERR α to evaluate the function of this receptor in animal models as well as determine the potential utility of ERR α ligands in human diseases. The lack of chemical probes to this drug target has hindered our ability to study the relationship between ERR α activity and diseases states and to launch the clinical translatability of this target. GSK4716 (**6**) (Fig. 1) was reported as an agonist of ERR β and ERR γ with no observed activity on ERR α [23]. In our hands, GSK4716 (**6**) showed very weak activity against ERR α , which prompted us to revisit this lead compound to identify ERR α / γ dual agonists. Herein we describe our probe of the structure activity relationships (SARs) of GSK4716 (**6**) through the chemical modification of rings A and B while maintaining the acyl hydrazone moiety to identify the structural requirements to promote selectivity toward the ERR α isoform.

2. Results and discussion

2.1. Chemistry

The synthesis of compounds **10–46** is illustrated in Scheme 1. The acyl hydrazides (**8**) were prepared from their corresponding methyl esters (**7**) through reaction with hydrazine in methanol under reflux. All acyl hydrazides (**8**) were obtained in quantitative yields and their identity were confirmed by comparing their melting points and mass to literature. The acyl

hydrazones (**10–46**) were synthesized by condensation of acyl hydrazides (**8**) with aldehydes (**9**) in ethanol in presence of catalytic amount of trifluoroacetic acid.

2.2. SAR study of acyl hydrazone derivatives

Synthesized compounds were screened in a cell-based (HEK293 cells) co-transfection assay using ERRE reporter construct and pcDNA3.1 ERR γ or pcDNA3.1 ERR α . Luciferase activity was measured using the Dual-Glo luciferase reporter assay system (Promega). The values indicated represent the means \pm S.E. from four independently transfected wells. EC₅₀ values for all described compounds were obtained by titration in an eleven-point dose response format. All compounds were screened against GSK4716 (**6**) as a reference compound for agonist activity. Compounds XCT790 (**3**), which is a potent and specific inverse agonist for ERR α , and 4-hydroxytamoxifen (4-OHT), which is a nonselective inverse agonist for ERR γ , were used as positive controls to identify inverse agonism activity.

Zuercher et al. [23] reported that the hydroxyl group or analogous hydrogen bond donor (HBD) group on ring A is required to obtain ERR γ activity. Recently, Lin et al. [24] showed that removing or repositioning this hydroxyl group led to significant decrease or even complete loss of ERR γ activity. 4-Isopropyl and 4-diethylamino groups were the optimal substituents at ring B to maintain ERR γ activity.

We started probing the SAR of GSK4716 (**6**) by removing both substituents at both rings A and B, which led to complete loss of activity against both ERR α and ERR γ (i.e. **10**). Then, we investigated the SAR of ring B while ring A was unsubstituted phenyl. ERR γ activity was regained upon introduction of 4-dimethylamino (i.e. **11**) or 4-chloro (i.e. **12**), but no ERR α activity was observed. Compound **12** was > 8-fold more potent than **11**. While hydroxyl group at the *ortho*-position of ring B was not tolerated (i.e. **13**) and the compound was inactive against both ERR α and ERR γ , compound **14** with hydroxyl group at the *para*-position showed weak activity against both isoforms and was more selective toward ERR γ (> 3-fold) (Table 1).

A methoxy group at *para*-position of ring B (i.e. **15**) enhanced the activity toward both ERR α and ERR γ but remained more selective toward ERR γ (\approx 3-fold). Compound **15** was \approx 2.66-fold more potent toward ERR α than **14**. Introduction of nitro group at the *ortho*-position of ring B (i.e. **16**) increased the potency toward ERR α > 6-fold if compared to **15** and \approx 17-fold if compared to **14**. Compound **16** remained more selective toward ERR γ over ERR α (1.6-fold). Moving the nitro group from *ortho*-position to *meta*- (i.e. **17**) or *para*-position (i.e. **18**) led to the loss of ERR α activity and significant decrease in ERR γ activity (Table 1). Docking of compound **16** in both ERR α and ERR γ resulted in a similar binding pose in both receptors. The ligand is involved in hydrophobic interactions with surrounding residues in the ligand binding pocket (LBP). The aromatic ring B makes π - π interactions with Tyr326 in ERR γ and π - π interactions with Phe328 in ERR α . The nitro group in this binding pose is oriented towards the inside of the cavity of ERR α , and involved in cation- π interactions with Phe328 which correspond to Ala272 in ERR γ (Fig. 2).

We then begin investigating the SAR of ring A while ring B remained fixed as an unsubstituted phenyl. When we introduced the hydroxyl group at *ortho*-position, we

obtained compound **19** that was active toward both ERR α ($EC_{50} = 0.619 \mu\text{M}$) and ERR γ ($EC_{50} = 0.468 \mu\text{M}$) with significant enhancement in selectivity toward ERR α ($EC_{50} \alpha/\gamma = 1.32$). Evans et al. [25] showed that compound DY162, which is an analogue of **19** with hydroxyl group at *para*-position of ring A, was ERR γ agonist with no activity toward ERR α .

Substituting ring A with chlorine at *para*-position led to identification of compound **20**, which was weakly active against ERR α ($EC_{50} = 1.714 \mu\text{M}$) and moderately potent against ERR γ ($EC_{50} = 0.790 \mu\text{M}$). Bromine (i.e. **21**) or nitro (i.e. **22**) groups were not tolerated at the same position. While both **21** and **22** maintained moderate ERR γ activity, they completely lost ERR α activity. Methyl substitution at *ortho*-position (i.e. **23**) showed a similar pattern with moderate activity toward ERR γ ($EC_{50} = 1.595 \mu\text{M}$) and no activity toward ERR α . Surprisingly, methyl substituent at *para*-position (i.e. **24**) enhanced the potency toward both ERR α ($EC_{50} = 0.209 \mu\text{M}$) and ERR γ ($EC_{50} = 0.194 \mu\text{M}$) significantly. Compound **24** was equipotent toward both isoforms ($EC_{50} \alpha/\gamma = 1.07$) (Table 1 and Fig. 3).

Molecular modeling of **24** in the active site of ERR γ show that ring B is making π - π interactions with Tyr326 and the NH makes a hydrogen bond with the carbonyl oxygen of the same residue (Fig. 4B). In ERR α , the predicted binding pose is a slightly tilted from the binding pose in ERR γ and the compound is predicted to make π - π interactions with Phe328 on helix 3 (H3) (Fig. 4A).

To further probe the SAR of this scaffold, we decided to assess the effect of having two different substituents at both rings A and B on the activity and selectivity toward ERR α and ERR γ (Table 2). When we introduced methyl group in *ortho*-position of ring A in **11**, we obtained compound **25**. Like **11**, compound **25** was inactive against ERR α and the potency toward ERR γ dropped > 4-fold. Introducing chlorine to the *para*-position of **12** gave compound **26**, which was inactive against both ERR isoforms. Interestingly, introducing hydroxyl group to the *ortho*-position of either ring A (i.e. **19**, Table 1) or ring B (i.e. **13**, Table 1) showed a very distinct pharmacological behavior. While **19** was moderately potent against both isoforms with slightly higher selectivity toward ERR γ , **13** was completely inactive against both isoforms. This further supports the importance of having a hydrogen bond donor (HBD) on ring A, especially in absence of any substituents at ring B, for the compound to have affinity toward ERRs. Introducing two hydroxyl groups to the *ortho*-position of both rings gave compound **27**, which was more potent toward ERR α ($EC_{50} = 0.378 \mu\text{M}$) than ERR γ ($EC_{50} = 1.645 \mu\text{M}$). Compound **27** is > 4-fold more selective toward ERR α over ERR γ ($EC_{50} \alpha/\gamma = 0.23$) (Table 2). This compound is expected to have poor pharmacokinetic properties because it is susceptible to metabolic clearance via glucuronidation or sulfonation of the two hydroxyl groups.

In ERR γ , **27** is predicted to make π - π interactions with Tyr326 that lies on the β -sheets region and hydrogen bonding interactions with Glu247. However, docking this compound in ERR α resulted in a docking pose where the molecule is slightly tilted to interact with Phe328 (Fig. 5). It is possible that this interaction contributes to selectivity of this compound towards ERR α . The hydroxyl group on ring A is predicted to make hydrogen

bonding interactions with Glu331 in ERR α . The amide group is making hydrogen bonding interaction with the backbone of Tyr326 in ERR γ and Phe328 in ERR α (Fig. 5).

The activity toward ERR α was lost completely when we replaced the hydroxyl group on ring A of **27** with chlorine atom in **28**. Compound **28** preserved activity toward ERR γ . On the contrary, **29** with methyl group in *ortho*-position of ring A was active toward both ERR α ($EC_{50} = 0.453 \mu\text{M}$) and ERR γ ($EC_{50} = 0.254 \mu\text{M}$). Ring B of **29** is predicted to make π - π interactions with Tyr326 in ERR γ . In ERR α , the same group is predicted to make π - π interactions with two aromatic side chains; Phe328 and Phe382. Moreover, the NH group of **29** is predicted to make hydrogen bonding interactions with the backbone of Tyr328 in ERR γ and Phe382 in ERR α (Fig. 6).

Moving hydroxyl group on ring B of **29** from *ortho*-position to *para*-position gave compound **30**, which was inactive toward both isoforms. Introducing chlorine or bromine in *para*-position of ring A while maintaining hydroxyl group in *ortho*-position of ring B, gave compounds **31** and **32**, respectively. These two compounds showed weak activity toward ERR α and ERR γ but were more selective toward ERR γ . Compound **33** with methyl group in the *para*-position of ring A showed good activity toward both ERR α ($EC_{50} = 0.483 \mu\text{M}$) and ERR γ ($EC_{50} = 0.235 \mu\text{M}$) (Table 2). Attempt to replace ring A with benzyl group gave compound **34** that was completely inactive against both isoforms. Compound **34** has no affinity toward ERRs most probably due to the extra flexibility gained by having methylene linker between ring A and the carbonyl group.

Compound **35** possess bromine in the *para*-position of ring A and methoxy in the *para*-position of ring B and showed good activity toward ERR α ($EC_{50} = 0.540 \mu\text{M}$) and ERR γ ($EC_{50} = 0.398 \mu\text{M}$) with good subtype selectivity ($EC_{50} \alpha/\gamma = 1.36$). The addition of bromine to ring A enhanced the subtype selectivity > 2-fold (*cf.* **15**; $EC_{50} \alpha/\gamma = 2.97$). However, in absence of methoxy group, compound **21** was inactive toward ERR α and very weak toward ERR γ . Compound **35** demonstrates the influence of additive effect and the interplay of substituents at ring A and ring B. Therefore, it is feasible to develop isoform selective modulators for ERR subtypes by having the right combination of substituents on both rings.

Both **18** (4-NO₂ on ring B) and **22** (4-NO₂ on ring A) were inactive toward ERR α and weakly active toward ERR γ . Introducing the two nitro groups simultaneously at both rings in compound **36** led to a switch in activity toward ERR α from agonism to inverse agonism. Compound **36** showed a weak decrease in the basal activity of ERR α ($IC_{50} = 8.116 \mu\text{M}$) compared to the ERR α potent inverse agonist **XCT790 (3)** ($IC_{50} = 0.175 \mu\text{M}$). Moreover, **36** was inactive against ERR γ . Since ERRs are constitutively active receptors, ligands that decrease their constitutive activity are identified as inverse agonists. Although the observed inverse agonism activity of this compound was very weak, it demonstrates that two electron-withdrawing groups at *para*-position of both rings are not tolerated. The compound lost activity toward both isoforms upon moving the nitro group on ring B from *para*-position (*i.e.* **36**) to *meta*-position (*i.e.* **37**). The agonistic activity was retained upon moving the nitro group on ring B from *meta*-position in **37** to *ortho*-position in **38** ($EC_{50} = 0.646 \mu\text{M}$ for ERR α , and $0.260 \mu\text{M}$ for ERR γ). Comparing **38** with nitro group in the *para*-position of

ring A to **16** that lacks nitro group on ring A, we noticed a slight decrease in the potency of **38** against ERR α (≈ 1.5 -fold) and insignificant change in potency against ERR γ . Moreover, subtype selectivity decreased by ≈ 1.5 -fold ($EC_{50} \alpha/\gamma = 1.6$ for **16** vs 2.48 for **38**). This decrease in activity and subtype selectivity toward ERR α is most likely due to the smaller size of the ligand binding pocket of ERR α , which prefers smaller ligands.

Finally, we decided to explore different substituents in lieu of ring B while maintaining the ring A as an unsubstituted phenyl ring (Table 3). Neither small alkyl substituent (i.e. **39**) nor phenylallyl analogs (i.e. **41** and **42**) were tolerated and these derivatives were inactive toward both ERR isoforms. Compound **42** with thiophene ring as a bioisostere of phenyl ring in **10** showed weak agonistic effect against both ERR isoforms and good subtype selectivity ($EC_{50} \alpha/\gamma = 1.78$). Despite the weak agonistic activity of **42**, replacement of phenyl ring with its bioisostere (i.e. thiophene) has changed the profile of **10** from completely inactive compound to an active compound (i.e. **42**) with acceptable isoform selectivity. The corresponding furan analogue (i.e. **43**) was inactive toward both isoforms. The 5-methyl substituted furan analogue (i.e. **44**), has weak ERR γ activity ($EC_{50} = 2.701 \mu\text{M}$) and no ERR α activity. The quinolin-2-ylmethylene benzo-hydrazide **45** was more potent against ERR α ($EC_{50} = 0.487 \mu\text{M}$) over ERR γ ($EC_{50} = 0.836 \mu\text{M}$). Surprisingly, the quinolin-4-ylmethylene benzohydrazide **46** showed weak inverse agonism behavior against ERR α ($IC_{50} = 4.578 \mu\text{M}$) in comparison to the ERR α potent inverse agonist **XCT790 (3)** ($IC_{50} = 0.175 \mu\text{M}$).

Our SAR data of developed agonists supported by molecular modelling show that removing the hydroxyl group at *para*-position of ring A in GSK4716 (**6**), which forms H-bond with Glu384 and avoiding using hydrogen bond donors at the same position reduced the selectivity toward ERR γ and enhanced the selectivity toward ERR α . The best functionalities at ring A were unsubstituted phenyl ring and phenyl ring substituted with Cl, Br, NO₂, Me (at *para*-position) or OH (at *ortho*-position). The best functionalities at ring B were unsubstituted phenyl ring, phenyl ring substituted with OH or NO₂ (at *ortho*-position), OMe (at *para*-position), and thiophene or quinoline heterocycles. Any spacer between ring A and carbonyl group or between ring B and azomethine group tend to abolish the activity.

Although ERR β is expressed in low levels in adult tissues and its postnatal expression is highly restricted, we have tested compounds **24**, **27**, **29**, **33**, and **42** against ERR β to address the activity of our synthesized agonists against this isoform (Table 4). All of our agonists activated ERR β , but there was no specific pattern corresponding to how it activate the other isoforms. Compounds **24** (Fig. 3) and **33** were more active toward ERR β than ERR α and ERR γ . Unlike **24** and **33**, compound **27** was more active toward ERR α than the two other isoforms (≈ 2 -folds higher than ERR β and > 4 -folds higher than ERR γ). Compound **29** was more active toward ERR α and ERR γ than ERR β . The activity of **42** toward ERR β was almost equal to ERR γ and 1.8-folds higher than ERR α .

2.3. Molecular modeling

We performed docking of selected compounds in the ligand binding pocket of ERR α and ERR γ . Molecular docking in ERR γ was performed using the ERR γ bound agonist

conformation (PDBID: 2GPP) [27]. There is no reported agonist bound conformation of ERR α and molecular docking of GSK4716 (**6**) to the agonist pocket in apo ERR α X-ray structure (PDID: 1XB7) was not possible initially because the pocket was occupied with the side chains of amino acid residues Phe328, Arg372 and Glu331 and there was not sufficient room to accommodate the ligand [28]. The amino acid residues in both pockets are similar and the agonist GSK4716 (**6**) is expected to bind in similar manner in both receptors with slight differences. In order to obtain an ERR α structure suitable for docking, we performed manual modeling of ERR α bound with the agonist GSK4716 (**6**) followed by refinement of the ligand bound complex by performing local optimization using Schrodinger/Prime [29]. The protein-ligand complex was validated using molecular dynamics simulations for 500 ns (data will be published in due course). The refined ERR α -ligand complex was used as the receptor in the docking calculations.

Molecular modelling using induced fit docking of compounds **16**, **24**, **27**, and **29** in the LBP of ERR α show that they have favorable binding modes where they make π - π interactions with Phe328, which corresponds to Ala272 in ERR γ . Moreover, the compounds tend to adopt a tilted confirmation to fit in the much smaller binding pocket of ERR α and make π - π interactions with Phe328 that originally occupies the available space in this binding pocket.

2.4. Gene expression

ERRs are the major transcriptional regulators that regulate key genes involved in energy metabolism within cells and tissues of high-energy demand. They regulate genes involved in carbohydrate and energy metabolism, lipid synthesis and fatty acid oxidation, mitochondrial activity and oxidative phosphorylation [20]. The agonistic effect of the best dual agonists (i.e. **16**, **24**, **27**, **29**, **35**, **38**, and **42**) was validated by measuring the changes in gene expression of four ERR target genes; PGC-1 α , PGC-1 β , CPT1 α and PDK4 (Fig. 7) in mouse myoblast cell line C2C12 at 1 μ M of tested compounds. The peroxisome proliferator-activated receptor- γ coactivator 1 α (PGC-1 α) and the peroxisome proliferator-activated receptor- γ coactivator 1 β (PGC-1 β) regulate several metabolic pathways and their activity is of great importance to achieve maximal mitochondrial biogenesis.

Compounds **24** and **42** were found to increase the mRNA levels of both PGC-1 α and PGC-1 β , while compound **35** increased the mRNA levels of PGC-1 α only. Carnitine palmitoyltransferase 1 α (CPT1 α) catalyzes the first step of long-chain fatty acid import into mitochondria, and its activity is believed to be rate limiting for β -oxidation of fatty acids. Compound **16** significantly increased the expression of CPT1 α . The pyruvate dehydrogenase kinase isozyme 4 (PDK4) play an important role in energy homeostasis and catalyzes the conversion of pyruvate to CoA. The transcription of PDK4 is controlled by both ERR α and ERR γ in hepatic cells and muscle. Compounds **16**, **24**, **35**, and **42** potently upregulated PDK4 transcription.

2.5. Cytotoxicity assay

Cell viability was assessed using FITC Annexin V/ Dead cell Apoptosis kit (Invitrogen) for flow cytometry according to the manufacturer's manual. Compounds **24**, **27**, **29**, and **42**

were tested at 1 and 10 μM . No signs of toxicity were observed for active compounds (Fig. 8).

2.6. In silico ADME evaluation

In order to evaluate the drug-likeness and to predict the absorption, distribution, metabolism, elimination and toxicity (ADMET) of some of the best identified modulators, we have calculated a set of molecular descriptors using QikProp program [30]. All evaluated compounds complied with Lipinski's Rule of Five and showed the desired molecular weight (MW), lipophilicity ($\log P$), number of hydrogen bond donors (HBD) and number of hydrogen bond acceptors (HBA) (Table 5). Compliance with Lipinski's Rule of Five indicate that these molecules have drug-like properties [31]. These compounds were also found to comply with Jorgensen's rule of 3 ($\text{Log}S_{\text{wat}}$, $\text{BIP}_{\text{Caco-2}}$, and number of primary metabolites) and are predicted to have oral bioavailability [32,33]. These compounds are predicted to have good aqueous solubility, cell permeability, and oral bioavailability (Table 5). The calculated apparent MDCK cell permeability, which mimic the BBB further suggests that these compounds have good cell permeability. Moreover, the estimated plasma-protein binding to human serum albumin ($\log K_{\text{HSA}}$) of these compounds are within the recommended range, which means that these compounds are predicted to circulate freely within the blood stream and can achieve high efficiency.

3. Conclusions

We were able to modulate the estrogen-related receptors subtype selectivity by converting an $\text{ERR}\beta/\gamma$ specific agonist, GSK4716 (**6**), into $\text{ERR}\alpha/\beta/\gamma$ pan agonists. Molecular modeling shows that the new pan agonists have favorable binding modes in both isoforms but have different conformations in the LBP of $\text{ERR}\alpha$. These ligands induce a new conformation in the cavity of $\text{ERR}\alpha$ where Phe328 is slightly displaced to accommodate the ligand and make π - π interactions with one of the two phenyl rings. The identified ligands increased the expression of ERR target genes, PGC-1 α , PGC-1 β , CPT1 α and PDK4 in mouse myoblast cell line C2C12. Compounds **24**, **27**, **29**, and **42** did not show signs of toxicity when tested at 1 and 10 μM . We identified the important structural requirements to enhance the selectivity toward $\text{ERR}\alpha$ and our future goal is to develop $\text{ERR}\alpha$ specific agonists to be used as chemical tools to validate $\text{ERR}\alpha$ as a putative target for treatment of neurodegenerative diseases like Alzheimer Disease.

4. Experimental

4.1. Chemistry

All starting materials were purchased from commercial suppliers and used without further purification. The purities of the final compounds were characterized by high-performance liquid chromatography (LC/MS) using a gradient elution program (Ascentis Express Peptide C18 column, acetonitrile/water 5/95/95/5, 5 min, 0.05% trifluoroacetic acid) and UV detection (254 nm). The purities of final compounds were 95% or greater. NMR spectra was recorded on a Bruker NMR 400 MHz Avance III spectrometer operating at 400 MHz for ^1H NMR

and 100 MHz for ^{13}C NMR. Chemical shifts are given in part per million (ppm) relative to the deuterated solvent residual peak, coupling constants J are given in Hertz.

4.1.1 General procedure for the preparation of hydrazides 8—Carboxylic acids **1a-g** (5 mmol) were heated under reflux in methanol (5 mL) for 2 h in presence of conc. H_2SO_4 (catalytic amount) with continuous stirring. The reaction was monitored by TLC till the acids were fully converted to the corresponding esters [Eluent: EtOAc/Hexanes (1:4)]. The reaction mixture was allowed to cool down to room temperature and hydrazine monohydrate 80% (20 mmol, 0.96 mL) was added slowly in an ice bath. The reaction was then warmed to room temperature and heated under reflux for another 1–2 h and followed by TLC till formation of hydrazide. The reaction mixture was kept at refrigerator till the product precipitated. All hydrazides were isolated in quantitative yields and in a pure form. Their melting points were in full agreement with the literature melting points of the same compounds.

4.1.2. General procedure for the preparation of hydrazones 10–46—A mixture of the appropriate hydrazides **8** (1 mmol) and the appropriate aldehyde **4a-j** (1.1 mmol) was refluxed in ethanol until the condensation was complete (monitored by TLC, 1–3 h). The reaction was allowed to cool to room temperature and the formed precipitate was filtered and washed with cold ethanol. The purity of most compounds was $\approx 98\%$ and in few cases the obtained solid was recrystallized from ethanol to give the desired product. All acyl hydrazones reported here are known compounds their identity were confirmed by comparing their melting points and mass to literature (See supporting information). ^1H and ^{13}C NMR spectra of most active compounds are described here.

4.1.2.1. (E)-N'-(2-Nitrobenzylidene)benzohydrazide (16) [34].: Pale yellow crystals, mp 222–224 °C, 89% yield. ^1H NMR (400 MHz, $\text{DMSO}-d_6$) δ 12.21 (s, 1H), 8.88 (s, 1H), 8.14 (d, $J = 7.3$ Hz, 1H), 8.08 (d, $J = 8.1$ Hz, 1H), 7.83 (d, $J = 7.2$ Hz, 2H), 7.83 (t, $J = 7.3$ Hz, 1H), 7.68 (t, $J = 7.6$ Hz, 1H), 7.63 – 7.50 (m, 3H); ^{13}C NMR (101 MHz, $\text{DMSO}-d_6$) δ 163.3, 148.3, 142.9, 133.7, 133.0, 132.0, 130.7, 128.8, 128.5, 127.9, 127.7, 124.7. LC/MS m/z : 270 $[\text{M}+\text{H}]^+$.

4.1.2.2. (E)-N'-Benzylidene-4-methylbenzohydrazide (24) [35].: White needles, mp 235–236 °C, 90% yield. ^1H NMR (400 MHz, $\text{DMSO}-d_6$) δ 11.78 (s, 1H), 8.47 (s, 1H), 7.84 (d, $J = 7.7$ Hz, 2H), 7.73 (d, $J = 6.3$ Hz, 2H), 7.50 – 7.41 (m, 3H), 7.33 (d, $J = 7.9$ Hz, 2H), 2.38 (s, 3H); ^{13}C NMR (101 MHz, $\text{DMSO}-d_6$) δ 162.9, 147.5, 141.8, 134.4, 130.5, 129.0, 128.8, 127.6, 127.0, 21.0. LC/MS m/z : 239 $[\text{M}+\text{H}]^+$.

4.1.2.3. (E)-2-Hydroxy-N'-(2-hydroxybenzylidene)benzohydrazide (27) [36].: White microcrystals, mp 265–267 °C, 85% yield. ^1H NMR (400 MHz, $\text{DMSO}-d_6$) δ 12.03 (s, 1H), 11.78 (s, 1H), 11.20 (s, 1H), 8.69 (s, 1H), 7.90 (d, $J = 7.1$ Hz, 1H), 7.57 (d, $J = 6.9$ Hz, 1H), 7.46 (t, $J = 7.7$ Hz, 1H), 7.32 (t, $J = 8.2$ Hz, 1H), 7.05 – 6.72 (m, 4H); ^{13}C NMR (101 MHz, $\text{DMSO}-d_6$) δ 164.5, 159.0, 157.50, 149.0, 134.0, 131.6, 129.5, 128.6, 119.4, 119.0, 118.6, 117.3, 116.5, 115.6. LC/MS m/z : 257 $[\text{M}+\text{H}]^+$.

4.1.2.4. (E)-N'-(2-Hydroxybenzylidene)-2-methylbenzohydrazide (29) [37].: White crystals, mp 163–165 °C, 50% yield. ¹H NMR (400 MHz, DMSO, two rotamers 4:1) δ 11.99 (s, 0.8H), 11.87 (s, 0.2H), 11.22 (s, 0.8H), 9.84 (s, 0.2H), 8.50 (s, 0.8H), 8.27 (s, 0.2H), 7.53 – 7.26 (m, 6H), 6.95 – 6.76 (m, 2H), 2.40 (s, 2.4H), 2.25 (s, 0.6H); ¹³C NMR (101 MHz, DMSO) δ 164.9, 157.4, 147.9, 136.1, 134.6, 131.4, 130.7, 130.2, 129.5, 127.6, 126.7, 125.7, 125.5, 119.4, 118.6, 116.4, 19.4. LC/MS *m/z*: 255 [M+H]⁺.

4.1.2.5. (E)-N'-(2-Hydroxybenzylidene)-4-methylbenzohydrazide (33) [38].: Yellow solid, mp 199–201 °C, 83% yield. ¹H NMR (400 MHz, DMSO-*d*₆) δ 12.01 (s, 1H), 11.30 (s, 1H), 8.60 (s, 1H), 7.82 (d, *J* = 7.9 Hz, 2H), 7.50 (d, *J* = 7.5 Hz, 1H), 7.35–7.25 (m, 3H), 6.89 (t, *J* = 8.1 Hz, 2H), 3.30 (s, 3H); ¹³C NMR (101 MHz, DMSO-*d*₆) δ 162.6, 157.5, 148.1, 142.1, 131.3, 129.9, 129.6, 129.1, 127.7, 119.3, 118.7, 116.4, 21.1. LC/MS *m/z*: 255 [M+H]⁺.

4.1.2.6. (E)-4-Bromo-N'-(4-methoxybenzylidene)benzohydrazide (35) [39].: White microcrystals, mp 129–131 °C, 89% yield. ¹H NMR (400 MHz, DMSO-*d*₆) δ 11.78 (s, 1H), 8.39 (s, 1H), 7.86 (d, *J* = 8.0 Hz, 2H), 7.71 (d, *J* = 8.0 Hz, 2H), 7.68 (d, *J* = 8.3 Hz, 2H), 7.02 (d, *J* = 8.3 Hz, 2H), 3.81 (s, 3H); ¹³C NMR (101 MHz, DMSO-*d*₆) δ 162.0, 160.9, 148.0, 132.6, 131.5, 129.7, 128.8, 126.8, 125.4, 114.4, 55.3. LC/MS *m/z*: 333 [M+H]⁺.

4.1.2.7. (E)-4-Nitro-N'-(2-nitrobenzylidene)benzohydrazide (38) [40].: White solid, mp 260–262 °C, 91% yield. ¹H NMR (400 MHz, DMSO-*d*₆) δ 12.47 (s, 1H), 8.90 (s, 1H), 8.38 (d, *J* = 8.6 Hz, 2H), 8.28 – 8.05 (m, 4H), 7.84 (t, *J* = 7.6 Hz, 1H), 7.71 (t, *J* = 7.6 Hz, 1H); ¹³C NMR (101 MHz, DMSO-*d*₆) δ 161.7, 149.4, 148.3, 144.2, 138.6, 133.8, 131.0, 129.3, 128.5, 128.1, 124.7, 123.7. LC/MS *m/z*: 315 [M+H]⁺.

4.1.2.8. (E)-N'-(Thiophen-2-ylmethylene)benzohydrazide (42) [37].: White crystals, mp 207–209 °C, 91% yield. ¹H NMR (400 MHz, DMSO-*d*₆) δ 11.77 (s, 1H), 8.64 (s, 1H), 7.86 (d, *J* = 7.5 Hz, 2H), 7.79 (d, *J* = 7.1 Hz, 1H), 7.57 – 7.38 (m, 4H), 7.11 (dd, *J* = 5.0, 3.6 Hz, 1H); ¹³C NMR (101 MHz, DMSO-*d*₆) δ 166.3, 143.4, 133.8, 131.4, 129.4, 128.9, 128.7, 128.3, 128.0, 127.4. LC/MS *m/z*: 231 [M+H]⁺.

4.2. Molecular modeling

Docking in ERR α and ERR γ was performed using the induced-fit docking module in Schrodinger to represent ligand-induced conformational changes [41–43]. Each ligand was initially docked using a softened potential (van der Waals radii scaling) of the ligand and the active site side chains. The scaling factors to soften the potentials of the receptors and ligands were set to 0.5 and the maximum number of poses was set to 20. The side chains of the residue within 5.0 Å of the ligand are refined along with the docked ligand with Prime using a continuum solvation based molecular mechanics model, via rotamer-based library optimizations of the amino acids side chain conformations [29]. The ligand is re-docked, using the standard precision algorithm implemented in Glide into the induced-fit receptor structures and re-minimized, and the final poses are rank ordered by the scoring function given by a linear combination of the Prime energy and GlideScore referred to as the IFDScore [42,44]. Images were made using Discovery Studio [45].

4.3. Cell culture

C2C12 cells, mouse myoblast cell line, were maintained in Dulbecco's modified Eagle's medium (DMEM) supplemented with 10% FBS and 1% L-Glutamine. The C2C12 cells were plated in 6 well dishes (Corning) with two and a half million cells per well and grew for 24 h until confluence is reached. The cells were then treated with either the drug in DMSO, or DMSO as the control at a concentration of 1 μ M or 10 μ M. All groups were tested in triplicates.

4.4. Cell viability assay

C2C12 cells were treated for 24 h with 1 μ M or 10 μ M of different compounds. After treatment, cells were harvested and stained for live/ dead cells using FITC Annexin V/ Dead Apoptosis Kit with FITC annexin V and PI, for Flow Cytometry (Invitrogen) according the manufacturer instruction. Cells were then analyzed by flow cytometry using BD Accuri c6 flow cytometer (BD Biosciences).

4.5. Gene expression

Cells were treated for 24 h with 10 μ M of different compounds. After treatment, cells were harvested and total RNA was extracted using RNeasy Mini Kit according the manufacturer instruction. Total RNA were quantified using NanoDrop and 1 μ g of total RNA was reverse transcript using qScript cDNA Synthesis Kit (QuantaBio) according the manufacturer instruction. Gene expression was assessed by qPCR using Sybr Select Master Mix (Applied Biotechnologies). All samples were run in duplicates and the analysis was completed by determining Ct values. The reference gene used was 36b4, a ribosomal protein gene.

Supplementary Material

Refer to Web version on PubMed Central for supplementary material.

Acknowledgments

We would like to thank Support & Development of Scientific Research Center (SDSRC) at Benha University (Egypt) for financial support for M.S. and S.G. This work was partially supported by the National Institute on Aging of the National Institutes of Health (United States) under Award Number R21AG065657 (to B.E.) and National Institute of Arthritis and Musculoskeletal and Skin Diseases (United States) under Award Number R01AR069280 (to T.B.).

References

- [1]. Giguère V, Yang N, Segui P, Evans RM, Identification of a new class of steroid hormone receptors, Nature 331 (1988) 91–94, 10.1038/331091a0. [PubMed: 3267207]
- [2]. Chen F, Zhang Q, McDonald T, Davidoff MJ, Bailey W, Bai C, Liu Q, Caskey CT, Identification of two hERR2-related novel nuclear receptors utilizing bioinformatics and inverse PCR, Gene 228 (1999) 101–109, 10.1016/S0378-1119(98)00619-2. [PubMed: 10072763]
- [3]. Eudy JD, Yao S, Weston MD, Ma-Edmonds M, Talmadge CB, Cheng JJ, Kimberling WJ, Sumegi J, Isolation of a gene encoding a novel member of the nuclear receptor superfamily from the critical region of usher syndrome type IIa at 1q41, Genomics 50 (1998) 382–384, 10.1006/geno.1998.5345. [PubMed: 9676434]

- [4]. Hong H, Yang L, Stallcup MR, Hormone-independent transcriptional activation and coactivator binding by novel orphan nuclear receptor ERR3, *J. Biol. Chem* 274 (1999) 22618–22626, 10.1074/jbc.274.32.22618.
- [5]. Heard DJ, Vissing H, Norby PL, Holloway J, Human ERR γ , a Third Member of the Estrogen Receptor-Related Receptor (ERR) Subfamily of Orphan Nuclear Receptors: Tissue-Specific Isoforms Are Expressed during Development and in the Adult, *Mol. Endocrinol* 14 (2000) 382–392, 10.1210/mend.14.3.0431. [PubMed: 10707956]
- [6]. Schlaeppi J-M, Fournier B, Bitsch F, Geiser M, Schilb A, Kallen J, Riou V, Strauss A, Filipuzzi I, Graham A, Evidence for Ligand-independent Transcriptional Activation of the Human Estrogen-related Receptor α (ERR α), *J. Biol. Chem* 279 (2004) 49330–49337, 10.1074/jbc.m407999200.
- [7]. Wang J, Fang F, Huang Z, Wang Y, Wong C, Kaempferol is an estrogen-related receptor α and γ inverse agonist, *FEBS Lett.* 583 (2009) 643–647, 10.1016/j.febslet.2009.01.030. [PubMed: 19171140]
- [8]. Stevens WC, Sapp DW, Busch BB, Zhou S, Mohan R, Martin R, Horlick RA, Ordentlich P, Identification of a Selective Inverse Agonist for the Orphan Nuclear Receptor Estrogen-Related Receptor α , *J. Med. Chem* 47 (2004) 5593–5596, 10.1021/jm049334f. [PubMed: 15509154]
- [9]. Kersual N, Chalbos D, Vanacker J-M, Bianco S, Lanvin O, Potentiation of ICI182,780 (Fulvestrant)-induced Estrogen Receptor- α Degradation by the Estrogen Receptor-related Receptor- α Inverse Agonist XCT790, *J. Biol. Chem* 282 (2007) 28328–28334, 10.1074/jbc.m704295200.
- [10]. Wang J, Wang Y, Wong C, Oestrogen-related receptor alpha inverse agonist XCT790 arrests A549 lung cancer cell population growth by inducing mitochondrial reactive oxygen species production, *Cell Prolif.* 43 (2010) 103–113, 10.1111/j.1365-2184.2009.00659.x. [PubMed: 20447055]
- [11]. Wu F, Wang J, Wang Y, Kwok TT, Kong SK, Wong C, Estrogen-related receptor α (ERR α) inverse agonist XCT-790 induces cell death in chemotherapeutic resistant cancer cells, *Chem. Biol. Interact* 181 (2009) 236–242, 10.1016/j.cbi.2009.05.008. [PubMed: 19464277]
- [12]. Chen L, Wong C, Estrogen-Related Receptor α Inverse Agonist Enhances Basal Glucose Uptake in Myotubes through Reactive Oxygen Species, *Biol. Pharm. Bull* 32 (2009) 1199–1203, 10.1248/bpb.32.1199. [PubMed: 19571385]
- [13]. Nie Y, Wong C, Suppressing the activity of ERR α in 3T3-L1 adipocytes reduces mitochondrial biogenesis but enhances glycolysis and basal glucose uptake, *J. Cell.Mol. Med* 13 (2009) 3051–3060, 10.1111/j.1582-4934.2008.00382.x. [PubMed: 18544047]
- [14]. Zuercher WJ, Stein RA, Hyatt SM, Willson TM, Orband-Miller LA, Lockamy EL, McDonnell DP, Miller AB, On the Intractability of Estrogen-Related Receptor α as a Target for Activation by Small Molecules, *J. Med. Chem* 50 (2007) 6722–6724, 10.1021/jm7012387. [PubMed: 18052088]
- [15]. Suetsugi M, Su L, Karlsberg K, Yuan Y-C, Chen S, Flavone and isoflavone phytoestrogens are agonists of estrogen-related receptors, *Mol. Cancer Res* 1 (2003) 981–991 <http://www.ncbi.nlm.nih.gov/pubmed/14638870>. [PubMed: 14638870]
- [16]. Peng L, Gao X, Duan L, Ren X, Wu D, Ding K, Identification of pyrido[1,2-*a*] pyrimidine-4-ones as new molecules improving the transcriptional functions of estrogen-related receptor α , *J. Med. Chem* 54 (2011) 7729–7733, 10.1021/jm200976s. [PubMed: 21958216]
- [17]. Griffett K, Solt LA, El-Gendy B-E-M, Kamenecka TM, Burris TP, A liver-selective LXR inverse agonist that suppresses hepatic steatosis, *ACS Chem. Biol* 8 (2013) 559–567, 10.1021/cb300541g. [PubMed: 23237488]
- [18]. Flaveny CA, Griffett K, El-Gendy B-E-M, Kazantzis M, Sengupta M, Amelio AL, Chatterjee A, Walker J, Solt LA, Kamenecka TM, Burris TP, Broad Anti-tumor Activity of a Small Molecule that Selectively Targets the Warburg Effect and Lipogenesis, *Cancer Cell.* 28 (2015) 42–56, 10.1016/j.ccell.2015.05.007. [PubMed: 26120082]
- [19]. El-Gendy B-E-M, Goher SS, Hegazy LS, Arief MMH, Burris TP, Recent Advances in the Medicinal Chemistry of Liver X Receptors, *J. Med. Chem* 61 (2018) 10935–10956, 10.1021/acs.jmedchem.8b00045.

- [20]. Goher SS, Griffett K, Hegazy L, Elagawany M, Arief MMH, Avdagic A, Banerjee S, Burris TP, Elgandy B, Development of novel liver X receptor modulators based on a 1,2,4-triazole scaffold, *Bioorganic Med. Chem. Lett* 29 (2019) 449–453, 10.1016/j.bmcl.2018.12.025.
- [21]. Khan PM, El-Gendy BEDM, Kumar N, Garcia-Ordonez R, Lin L, Ruiz CH, Cameron MD, Griffin PR, Kamenecka TM, Small molecule amides as potent ROR- γ selective modulators, *Bioorganic Med. Chem. Lett* 23 (2013) 532–536, 10.1016/j.bmcl.2012.11.025.
- [22]. Banerjee S, Wang Y, Solt LA, Griffett K, Kazantzis M, Amador A, El-Gendy BM, Huitron-Resendiz S, Roberts AJ, Shin Y, Kamenecka TM, Burris TP, Pharmacological targeting of the mammalian clock regulates sleep architecture and emotional behaviour, *Nat. Commun* 5 (2014), 10.1038/ncomms6759.
- [23]. Willson TM, Collins JL, Miller AB, Zuercher WJ, Orband-Miller LA, Chao EYH, Gaillard S, McDonnell DP, Jones DG, Shearer BG, Identification and Structure–Activity Relationship of Phenolic Acyl Hydrazones as Selective Agonists for the Estrogen-Related Orphan Nuclear Receptors ERR β and ERR γ , *J. Med. Chem* 48 (2005) 3107–3109, 10.1021/jm050161j. [PubMed: 15857113]
- [24]. Lin H, Doebelin C, Patouret R, Garcia-Ordonez RD, Ra Chang M, Dharmarajan V, Bayona CR, Cameron MD, Griffin PR, Kamenecka TM, Design, synthesis, and evaluation of simple phenol amides as ERR γ agonists, *Bioorganic Med. Chem. Lett* 28 (2018) 1313–1319, 10.1016/j.bmcl.2018.03.019.
- [25]. Evans RM, Downes M, Atkins A, Yu RT, Ahmadian M, Estrogen Related Receptor Gamma (Errgamma) Enhances And Maintains Brown Fat Thermogenic Capacity, US20180207114, 2018.
- [26]. Makarenko AS, Mauri A, Prokopenko VV, Tanchuk VY, Todeschini R, Ertl P, Tetko IV, Radchenko EV, Zefirov NS, Gasteiger J, Palyulin VA, Livingstone D, Virtual Computational Chemistry Laboratory – Design and Description, *J. Comput. Aided. Mol. Des* 19 (2005) 453–463, 10.1007/s10822-005-8694-y. [PubMed: 16231203]
- [27]. Wang L, Zuercher WJ, Consler TG, Lambert MH, Miller AB, Orband-Miller LA, McKee DD, Willson TM, Nolte RT, X-ray crystal structures of the estrogen-related receptor- γ ligand binding domain in three functional states reveal the molecular basis of small molecule regulation, *J. Biol. Chem* 281 (2006) 37773–37781, 10.1074/jbc.M608410200.
- [28]. Kallen J, Schlaeppi J-M, Bitsch F, Filipuzzi I, Schilb A, Riou V, Graham A, Strauss A, Geiser M, Fournier B, Evidence for Ligand-independent Transcriptional Activation of the Human Estrogen-related Receptor α (ERR α), *J. Biol. Chem* 279 (2004) 49330–49337, 10.1074/jbc.m407999200.
- [29]. Schrödinger Release 2020–1: Induced Fit Docking protocol; Glide, Schrödinger, LLC, New York, NY, 2020; Prime, Schrödinger, LLC, New York, NY, 2020., (n.d.).
- [30]. Schrödinger Release 2020–1: QikProp, Schrödinger, LLC, New York, NY, 2020., (2020).
- [31]. Lipinski CA, Lombardo F, Dominy BW, Feeney PJ, Experimental and computational approaches to estimate solubility and permeability in drug discovery and development settings, *Adv. Drug Deliv. Rev* 46 (2001) 3–26, 10.1016/S0169-409X(00)00129-0. [PubMed: 11259830]
- [32]. Jorgensen WL, Duffy EM, Prediction of drug solubility from structure, *Adv. Drug Deliv. Rev* 54 (2002) 355–366, 10.1016/S0169-409X(02)00008-X. [PubMed: 11922952]
- [33]. Jorgensen WL, Duffy EM, Prediction of drug solubility from Monte Carlo simulations, *Bioorganic Med. Chem. Lett* 10 (2000) 1155–1158, 10.1016/S0960-894X(00)00172-4.
- [34]. Rajput AP, Rajput SS, Synthesis of benzaldehyde substituted (phenylcarbonyl) hydrazones and their formylation using Vilsmeier-Haack reaction, *Int. J. PharmTech Res* 1 (2009) 1605–1611.
- [35]. Gillis BT, Schimmel KF, Peracetic acid oxidation of hydrazones. I. Aromatic aldehyde alkylhydrazones, *J. Org. Chem* 27 (1962) 413–417, 10.1021/jo01049a017.
- [36]. Patel HS, Patel SJ, Synthesis and biological activity of 2-hydroxy-N-(5-methylene-4-oxo-2-arylthiazolidin-3-yl)-benzamide, *Phosphorus, Sulfur Silicon Relat. Elem* 185 (2010) 1632–1639, 10.1080/10426500903176521.
- [37]. Ainscough EW, Brodie AM, Denny WA, Finlay GJ, Gothe SA, Ranford JD, Cytotoxicity of salicylaldehyde benzoylhydrazone analogs and their transition metal complexes: quantitative structure–activity relationships, *J. Inorg. Biochem* 77 (1999) 125–133, 10.1016/S0162-0134(99)00131-2. [PubMed: 10643654]

- [38]. Edward JT, Gauthier M, Chubb FL, Ponka P, Synthesis of new acylhydrazones as iron-chelating compounds, *J. Chem. Eng. Data* 33 (1988) 538–540, 10.1021/je00054a044.
- [39]. Kumar P, Narasimhan B, Ramasamy K, Mani V, Mishra RK, Abdul Majeed AB, Synthesis, Antimicrobial, Anticancer Evaluation and QSAR Studies of 3/4-Bromo Benzohydrazide Derivatives, *Curr. Top. Med. Chem. (Sharjah, United Arab Emirates)* 15 (2015) 1050–1064, 10.2174/156802661511150408111252.
- [40]. Desai KG, Desai KR, Synthesis of some novel pharmacologically active Schiff bases using microwave method and their derivatives formazans by conventional method., *Indian J. Chem. Sect. B Org. Chem. Incl. Med. Chem* 44B (2005) 2097–2101.
- [41]. Farid R, Day T, Friesner RA, Pearlstein RA, New insights about HERG blockade obtained from protein modeling, potential energy mapping, and docking studies, *Bioorganic Med. Chem* 14 (2006) 3160–3173, 10.1016/j.bmc.2005.12.032.
- [42]. Sherman W, Day T, Jacobson MP, Friesner RA, Farid R, Novel procedure for modeling ligand/receptor induced fit effects, *J. Med. Chem* 49 (2006) 534–553, 10.1021/jm050540c. [PubMed: 16420040]
- [43]. Sherman W, Beard HS, Farid R, Use of an induced fit receptor structure in virtual screening, *Chem. Biol. Drug Des* 67 (2006) 83–84, 10.1111/j.1747-0285.2005.00327.x. [PubMed: 16492153]
- [44]. Clark AJ, Tiwary P, Borrelli K, Feng S, Miller EB, Abel R, Friesner RA, Berne BJ, Prediction of Protein-Ligand Binding Poses via a Combination of Induced Fit Docking and Metadynamics Simulations, *J. Chem. Theory Comput* 12 (2016) 2990–2998, 10.1021/acs.jctc.6b00201. [PubMed: 27145262]
- [45]. BIOvIA DS Discovery studio modeling environment. San Diego, Dassault Systemes, Release, 4. 2020.

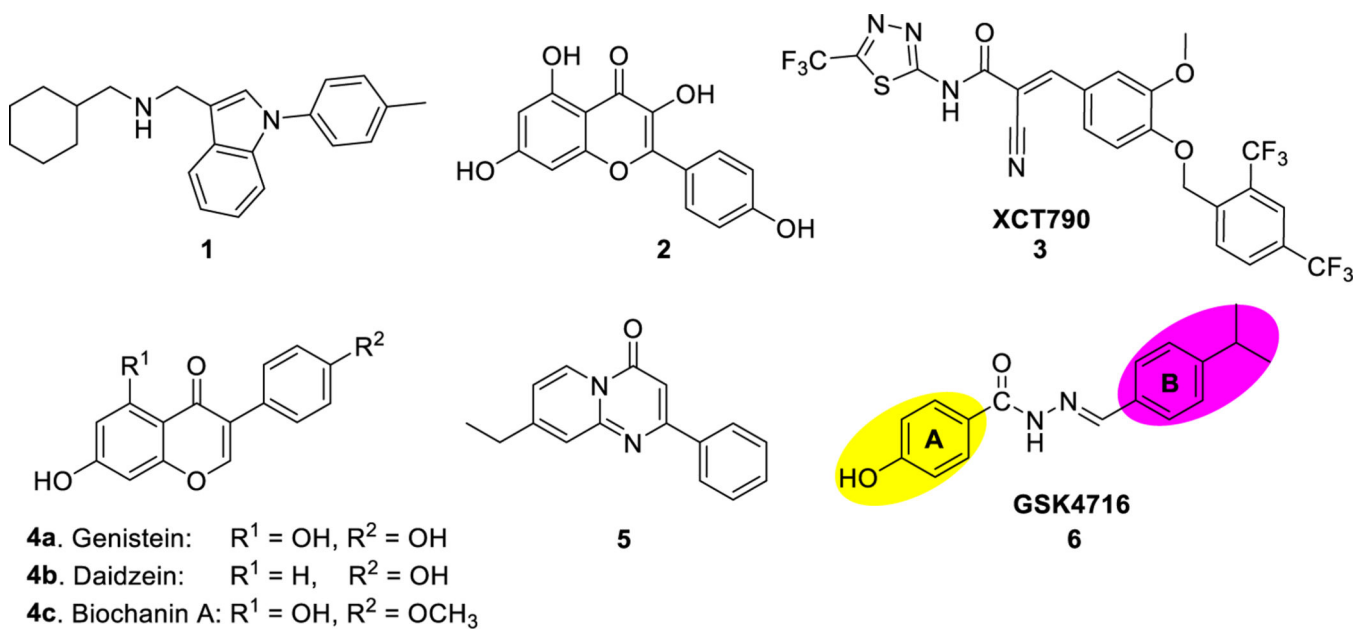
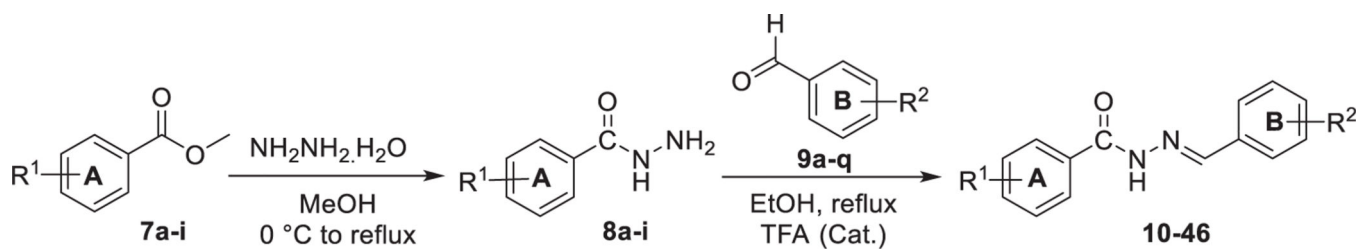


Fig. 1.
Examples of ERR α modulators.



Scheme 1.
Synthesis of *N*-acyl hydrazones **10-46**.

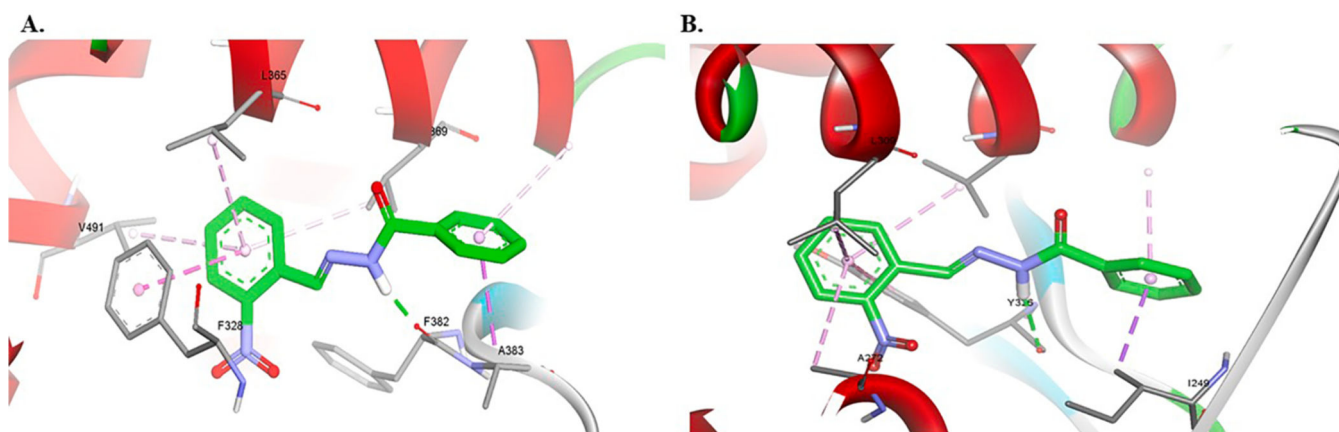


Fig. 2. Computational docking of **16** in ERR α (A) and ERR γ (B). Hydrogen bonds are shown as green dashed lines and hydrophobic interactions are shown as purple dashed lines. (For interpretation of the references to colour in this figure legend, the reader is referred to the web version of this article.)

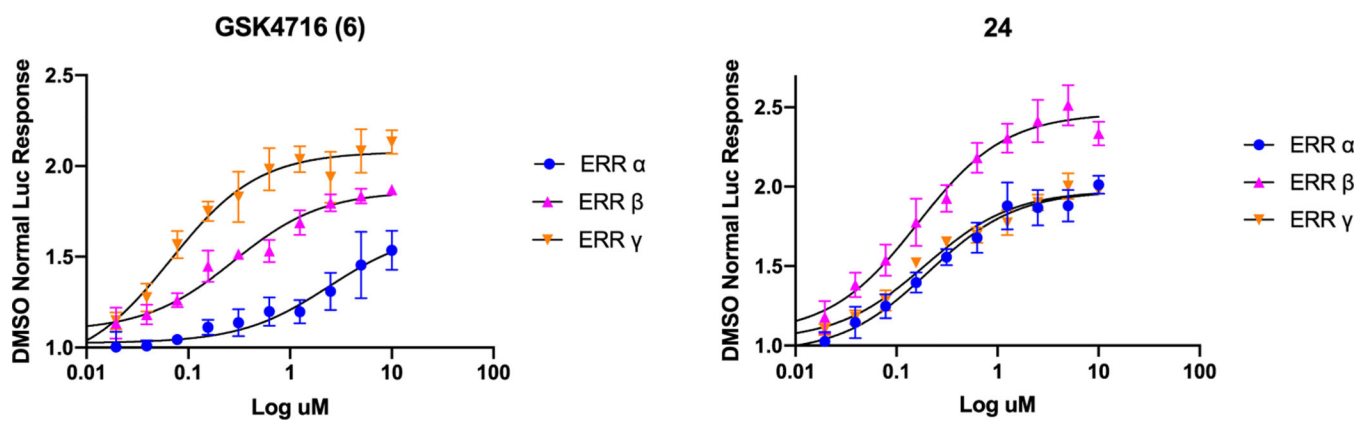


Fig. 3.
A cell-based co-transfection assay using ERR responsive luciferase reporter for GSK4716
(6) and 24.

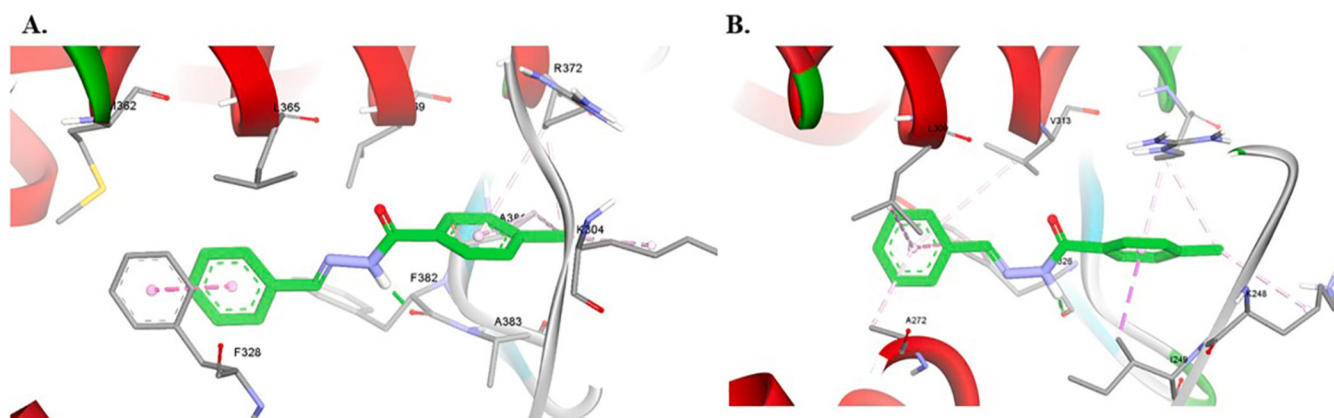


Fig. 4. Computational docking of **24** in ERR α (A) and ERR γ (B). Hydrogen bonds are shown as green dashes lines and hydrophobic interactions are shown as purple dashed lines. (For interpretation of the references to colour in this figure legend, the reader is referred to the web version of this article.)

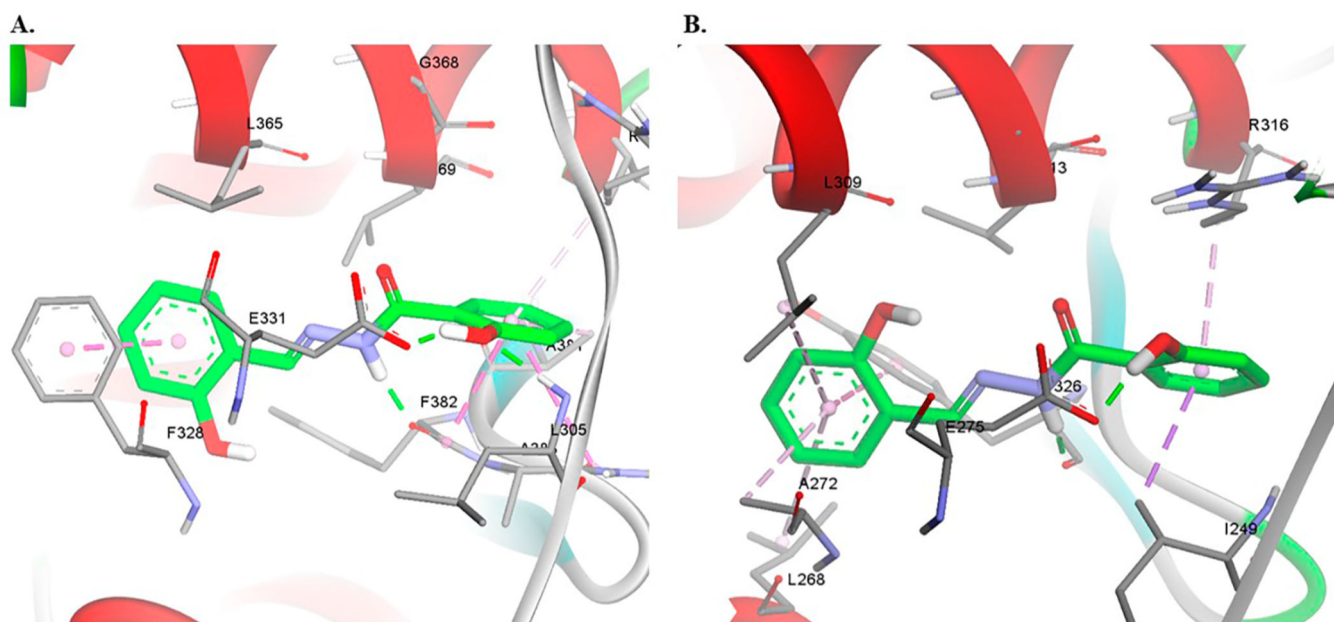


Fig. 5. Computational docking of **27** in ERR α (A) and ERR γ (B). Hydrogen bonds are shown as green dashed lines and hydrophobic interactions are shown as purple dashed lines. (For interpretation of the references to colour in this figure legend, the reader is referred to the web version of this article.)

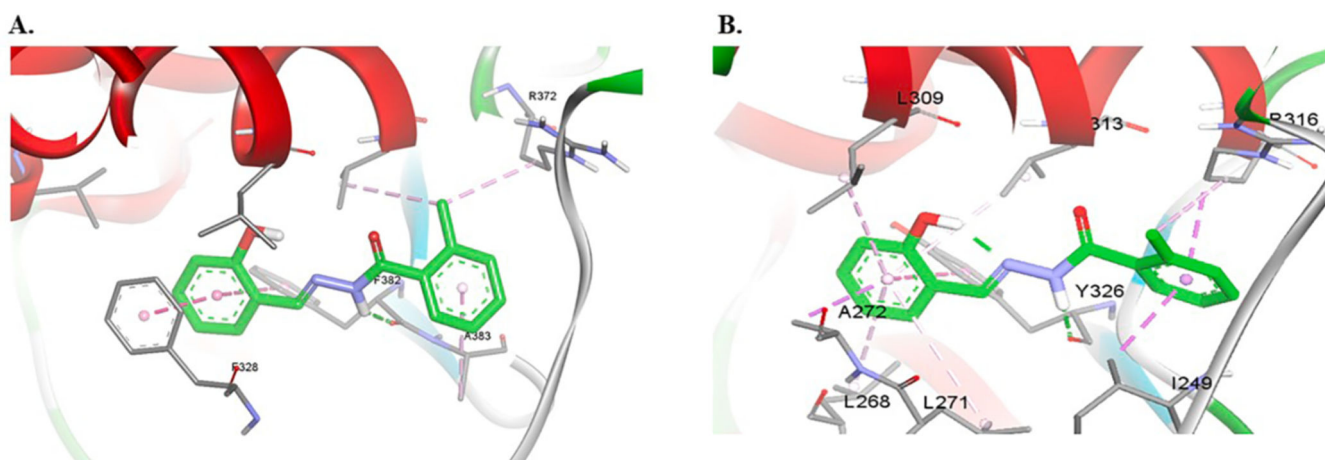


Fig. 6. Computational docking of **29** in ERR α (A) and ERR γ (B). Hydrogen bonds are shown as green dashed lines and hydrophobic interactions are shown as purple dashed lines. (For interpretation of the references to colour in this figure legend, the reader is referred to the web version of this article.)

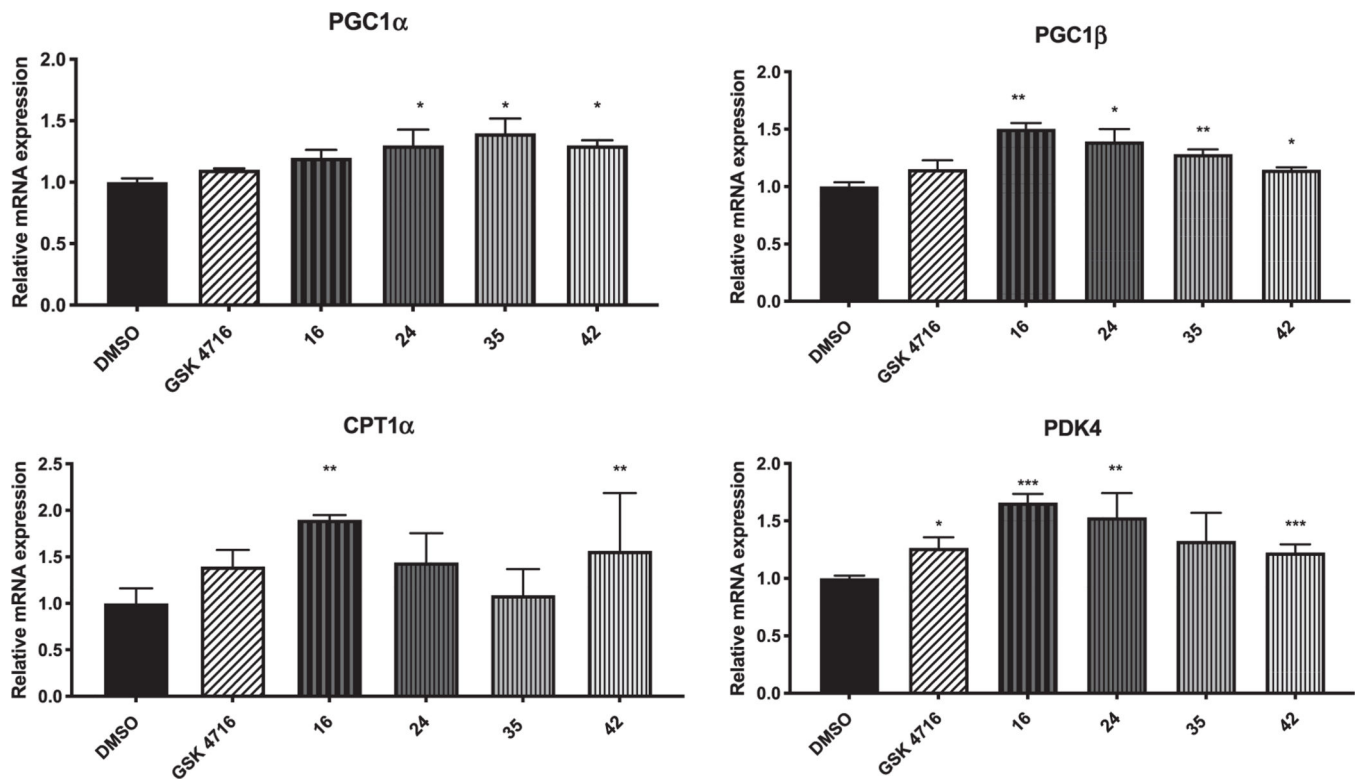


Fig. 7.
Normalized mRNA expression of PGC-1 α , PGC-1 β , CPT1 α and PDK4 with 16, 24, 35, and 42 in muscle cells.

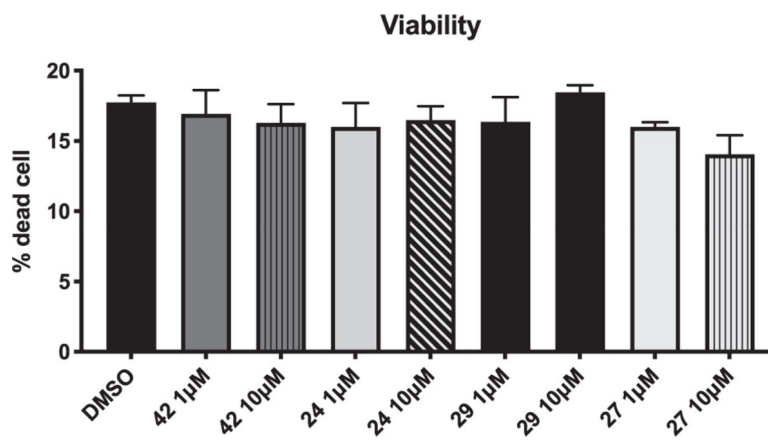


Fig. 8.
Cell viability of 24, 27, 29, and 42.

Author Manuscript

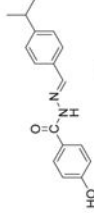
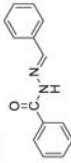
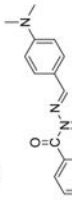
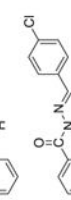
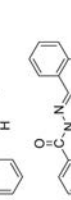
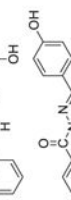
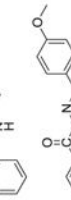
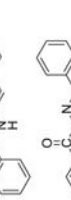
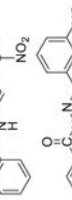

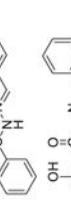
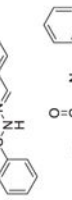
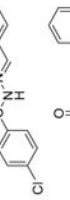
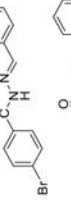
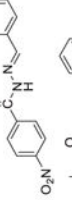
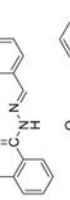
Author Manuscript

Author Manuscript

Author Manuscript

Table 1

***In vitro* ERR α and ERR γ agonistic activities of 10–24.**

Comp.	Structure	ERR α EC ₅₀ (μ M)	ERR γ EC ₅₀ (μ M)	EC ₅₀ α/γ	aLog P ^c
GSK4716 (6)		2.410	0.067	35.97	4.23
10		i.a.	i.a.	–	2.56
11		i.a.	1.704	–	3.14
12		i.a.	0.197	–	3.21
13		i.a.	i.a.	–	3.11
14		7.267	2.219	3.27	3.08
15		2.733	0.919	2.97	2.66
16		0.430	0.268	1.60	2.62
17		9.464	6.446	1.47	2.62
18		i.a.	1.839	–	2.62
19		0.619	0.468	1.32	3.12
20		1.714	0.790	2.17	3.21
21		i.a.	3.987	–	3.23
22		i.a.	1.830	–	2.63
23		i.a.	1.595	–	2.78
24		0.209	0.194	1.07	2.82

ALOGPS 2.1, molecular property prediction [26]. i.a. = inactive

Author Manuscript

Author Manuscript

Author Manuscript

Author Manuscript

Author Manuscript

Author Manuscript

Author Manuscript

Author Manuscript

Table 2

***In vitro* ERR α and ERR γ agonistic activities of 25–38.**

Comp.	Structure	ERR α EC ₅₀ (μ M)	ERR γ EC ₅₀ (μ M)	EC ₅₀ α/γ	dLog P ^a
GSK4716 (6)		2.410	0.067	35.97	4.23
25		i.a.	7.268	–	3.18
26		i.a.	i.a.	–	3.84
27		0.378	1.645	0.23	2.79
28		i.a.	1.42	–	3.79
29		0.453	0.254	1.78	3.35
30		i.a.	i.a.	–	3.35
31		3.347	2.804	1.19	3.76
32		2.054	0.6748	3.04	3.86
33		0.483	0.235	2.06	3.37
34		i.a.	i.a.	–	2.70
35		0.540	0.398	1.36	3.32
36		8.116 (Inverse agonist)	i.a.	–	3.13
37		i.a.	i.a.	–	3.10
38		0.646	0.260	2.48	3.10

Table 3

In vitro ERR α and ERR γ agonistic activities of 39–46.

Comp.	Structure	ERR α EC ₅₀ (μ M)	ERR γ EC ₅₀ (μ M)	EC ₅₀ α/γ	dLog P ^a
GSK4716 (6)		2.410	0.067	35.97	4.23
39		i.a.	i.a.	–	1.50
40		i.a.	i.a.	–	3.42
41		i.a.	i.a.	–	3.81
42		2.158	1.213	1.78	2.79
43		i.a.	i.a.	–	2.25
44		i.a.	2.701	–	2.54
45		0.487	0.836	0.58	2.84
46		4.578 (Inverse agonist)	i.a.	–	2.54

Table 4*In vitro* ERR β agonistic activities of **24**, **27**, **29**, **33**, and **42**.

	GSK4716 (6)	24	27	29	33	42
ERR β EC ₅₀ (μ M)	0.280	0.162	0.772	0.583	0.123	1.193

Author Manuscript

Author Manuscript

Author Manuscript

Author Manuscript

Table 5

Calculated molecular descriptors for prediction of ADME properties for **16**, **24**, **27**, **29**, **35**, and **42**.

Descriptors/Properties	^a MW (Da)	^b HBD	^c HBA	^d PSA	^e LogP _{o/w}	^f LogSwat (moles/liter)
Range for 95% of known Drugs	130.0 to 725.0	0 to 6	2.0 to 20.0	7.0 to 200.0	-2.0 to 6.5	-6.5 to 0.5
16	269.26	1	3.5	93.04	2.81	-3.93
24	238.29	1	2.5	49.78	3.85	-4.46
27	256.26	2	3	89.93	2.52	-3.51
29	254.29	2	3.25	68.23	3.08	-4.24
35	333.18	1	3.25	57.98	4.06	-4.95
42	230.28	1	2.5	48.35	2.90	-3.34
Properties	^g %Human oral absorption	^h Log B/B	ⁱ BIP _{Caco-2} (nm/sec)	^j MDCK	^k #metab	^l LogK _{HSA}
Range for 95% of known Drugs	< 25% is poor	-3.0 to 1.2	< 25 poor, >500 great	<25 poor, > 500 great	1.0 to 8.0	-1.5 to 1.5
16	88	-1.26	319	144	1	0.13
24	100	-0.34	2230	1177	1	0.34
27	87	-1.25	353	160	2	0.02
29	100	-0.67	1170	586	2	0.11
35	100	-0.23	2230	3120	1	0.34
42	100	-0.29	1891	1330	1	0.05

^aMolar weight;

^bNumber of hydrogen bonds donated by the molecule;

^cNumber of hydrogen bonds accepted by the molecule,

^dPolar surface area;

^eLogarithm of partitioning coefficient between *n*-octanol and water phases;

^fLogarithm of aqueous solubility;

^gPredicted human oral absorption on a 0–100% scale, based on a multiple linear regression model;

^hLogarithm of predicted blood/brain barrier partition coefficient;

ⁱPredicted apparent Caco-2 cell membrane permeability in Boehringer–Ingelheim scale;

Author Manuscript

Author Manuscript

Author Manuscript

Author Manuscript

P_x Predicted apparent MDCK cell permeability;

N_x Number of likely metabolic reactions;

L_x Logarithm of predicted binding constant to human serum albumin.